JACS
JOURNAL OF THE AMERICAN CHEMICAL SOCIETY
Communication
pubs.acs.org/JACS

Cocoon-Like Self-Degradable DNA Nanoclew for Anticancer Drug Delivery

Wujin Sun,[†,‡] Tianyue Jiang,[†,‡,§] Yue Lu,[†,‡] Margaret Reiff,[†] Ran Mo,[†,‡,§,*] and Zhen Gu*[,†,‡]

[†]Joint Department of Biomedical Engineering, University of North Carolina at Chapel Hill and North Carolina State University, Raleigh, North Carolina 27695, United States

[‡]Division of Molecular Pharmaceutics and Center for Nanotechnology in Drug Delivery, UNC Eshelman School of Pharmacy, University of North Carolina at Chapel Hill, Chapel Hill, North Carolina 27599, United States

[§]State Key Laboratory of Natural Medicines and Jiangsu Key Laboratory of Drug Discovery for Metabolic Diseases, Center of Drug Discovery, China Pharmaceutical University, Nanjing 210009, China

Supporting Information

ABSTRACT: A bioinspired cocoon-like anticancer drug delivery system consisting of a deoxyribonuclease (DNase)-degradable DNA nanoclew (NCl) embedded with an acid-responsive DNase I nanocapsule (NCa) was developed for targeted cancer treatment. The NCl was assembled from a long-chain single-stranded DNA synthesized by rolling-circle amplification (RCA). Multiple GC-pair sequences were integrated into the NCl for enhanced loading capacity of the anticancer drug doxorubicin (DOX). Meanwhile, negatively charged DNase I was encapsulated in a positively charged acid-degradable polymeric nanogel to facilitate decoration of DNase I into the NCl by electrostatic interactions. In an acidic environment, the activity of DNase I was activated through the acid-triggered shedding of the polymeric shell of the NCa, resulting in the cocoon-like self-degradation of the NCl and promoting the release of DOX for enhanced therapeutic efficacy.

Self-assembled DNA nanostructures have been developed with precisely controlled size and architecture.[1] Because of DNA's intrinsic biocompatibility and degradability, DNA nanostructures hold tremendous promise for drug delivery. Numerous cargoes, including small-molecule drugs,[2] small interfering RNA (siRNA),[1a,3] the immunostimulatory oligonucleotide CpG,[4] photosensitizers,[5] and proteins,[1b] have been successfully delivered intracellularly by DNA nanocarriers. Moreover, DNA-based carriers can be readily functionalized either by hybridizing a targeting moiety onto the nanostructure[1a] or programming a targeting aptamer into the DNA chain[1b,c] for targeted drug delivery. Despite these advances, strategies utilizing DNA scaffolds for on-demand drug delivery in a stimuli-responsive fashion,[6] instead of passive release,[7] still remain elusive. We have recently reported an adenosine triphosphate (ATP)-responsive formulation incorporating short DNA strands (with ATP's aptamer) loaded with doxorubicin (DOX), an anticancer drug.[8] The enhanced drug release inside cancer cells triggered by a high ATP level was validated. However, this design is limited by a complicated formulation process and relatively low drug loading capacity.

We herein describe a bioinspired drug delivery carrier in which a cocoon-like DNA nanocomposite is integrated with "caged worm" deoxyribonuclease (DNase) to achieve self-degradation for promoting drug release inside cells (Figure 1). The DNA structure is based on a "nanoclew" (denoted as NCl) that is "woven" by rolling-circle amplification (RCA) [Scheme S1 in the Supporting Information (SI)], the product of which is often applied in biodetection.[9] Multiple GC-pair sequences are integrated into the NCl to enhance the loading capacity of

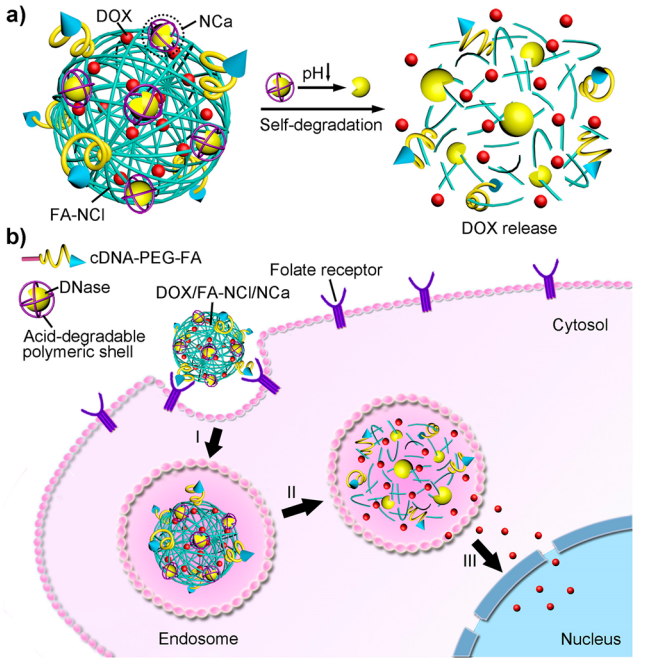

Figure 1. (a) Main components of the cocoon-like self-degradable DNA nanoclew, consisting of DOX/FA-NCl/NCa, and acid-triggered DOX release. (b) Schematic illustration of efficient delivery of DOX by DOX/FA-NCl/NCa to nuclei for cancer therapy: (I) internalization in endosomes; (II) pH-triggered degradation of the NCl for DOX release; (III) accumulation of DOX in cell nuclei.

Received: August 26, 2014
Published: October 13, 2014

   dx.doi.org/10.1021/ja5088024 | J. Am. Chem. Soc. 2014, 136, 14722−14725

DOX.[8] To facilitate self-assembly, a palindromic sequence is incorporated into the template. To enable degradation of NCl, DNase I is encapsulated into a single-protein-based nanocapsule (denoted as NCa) with a positively charged thin polymeric shell that is cross-linked by acid-degradable cross-linkers using interfacial polymerization (Figure 1a).[10] Furthermore, to achieve tumor-targeting delivery of DOX, folic acid (FA) is conjugated to an NCl complementary DNA (cDNA) oligomer followed by hybridization to the DNA NCl. The positively charged NCa can be embedded into the NCl via electrostatic interactions to form the DOX-loaded self-degradable DNA scaffold (designated as DOX/FA-NCl/NCa). The polymeric capsule cages the activity of DNase I at physiological pH, causing DOX to be retained in the NCl. When DOX/FA-NCl/NCa is internalized by cancer cells and enters the acidic endolysosome, the polymeric shell of NCa degrades and is shed from DNase I. This results in the immediate rejuvenation of DNase I, which rapidly degrades NCl, thereby releasing the encapsulated DOX for enhanced anticancer efficacy (Figure 1b). This formulation represents a novel stimuli-responsive drug delivery system, the trigger of which is preloaded with the delivery vehicle and can be activated by the cellular environment.

To validate our assumption, we first synthesized the DNA NCl by RCA (the sequence is shown in Table S1 in the SI). Cyclization of the single-stranded DNA (ssDNA) template was confirmed by its resistance to Exonuclease I, and RCA products with various molecular weights were amplified from the circular ssDNA template (Figure S1 in the SI). NCl exhibited high stability after incubation with culture medium containing fetal bovine serum (FBS) (10% v/v) for up to 48 h (Figure S1c). The synthesized ssDNA self-assembled into the three-dimensional clew-like structure with an average particle size of 150 nm (Figure 2a). Intercalation of DOX into NCl was monitored via the fluorescence intensity of the DOX solution, which significantly declined when NCl was added as a result of self-quenching[8] of DOX upon interacting with the NCl (Figure S2). The DOX loading was also assessed (Figure S3). It was found that at a mass ratio of 2.3, NCl showed a maximum DOX-loading capacity of 66.7%, and 86.5% of the added DOX was entrapped in the obtained NCl.

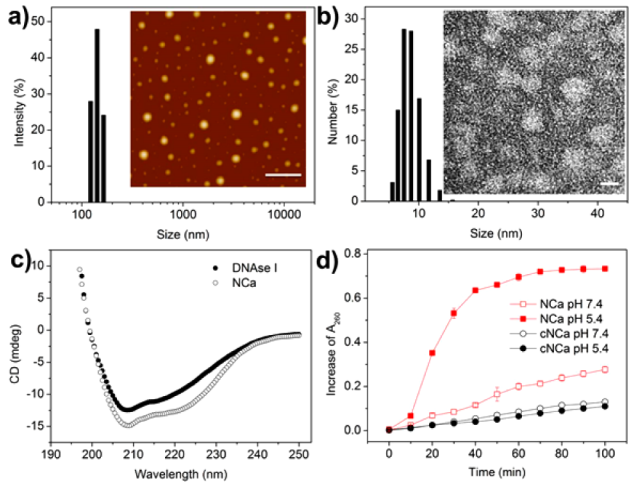

Figure 2. (a) Hydrodynamic size of NCl as determined by dynamic light scattering (DLS). Inset: atomic force microscopy (AFM) image of NCl. The scale bar is 500 nm. (b) Hydrodynamic size of NCa. Inset: transmission electron microscopy (TEM) image of NCa. The scale bar is 10 nm. (c) Circular dichroism (CD) spectra of native DNase I and NCa. (d) DNA-degrading activities of NCa and cNCa at pH 7.4 and 5.4. Bars represent mean ± standard deviation (n = 3).

Both native DNase I and the obtained NCl had negatively charged surfaces (Table S2). To integrate them together, DNase I was encapsulated in a positively charged polymeric single-protein nanogel by means of in situ free-radical polymerization,[10b] which encapsulated DNase I into a capsule with the ζ potential converted from −9 to +3 mV. Monodispersed NCa was obtained with an average particle size of 8.0 nm, which is larger than the size of the native DNase I (4.2 nm) (Figure 2b). Encapsulating DNase I in the capsule had no impact on its secondary structure (Figure 2c), and acid-responsive degradation[11] of NCa was observed (Figure S4). Glycerol dimethacrylate (GDA), the pH-responsive cross-linker in NCa, is stable at physiological pH but degradable at a lower pH,[10a] NCa degradation was observed after incubation at pH 5.4 for 2 h. The particle size of NCa was remarkably decreased at pH 5.4 compared with that at pH 7.4.

To further substantiate the pH-responsive DNA-degrading capability of NCa, a nondegradable DNase I capsule (cNCa) prepared with a nondegradable cross-linker, methylenebis-(acrylamide), in place of GDA was used as a control. The pH responsiveness of NCa was further confirmed by testing the enzymatic activity of DNase I (Figure 2d). Because of the nondegradability of cNCa, the polymeric shell of cNCa impeded the DNase I activity at both pH 7.4 and 5.4. However, NCa showed significantly higher DNase I activity at pH 5.4 than that at pH 7.4.

Next, we mixed negatively charged NCl with positively charged NCa to form homogeneous NCl/NCa complexes (PDI = 0.24 ± 0.02). The NCl/NCa assembly was observed by the colocalization of the fluorescence signals of DOX (red) in DOX/NCl and Alexa Fluor 488 (AF488) (green) in AF488-modified NCa (Figure S5). The NCl/NCa assembly increased the average hydrodynamic size of NCl from 150 to 180 nm, and the NCl ζ potential was converted from negative to positive (Figure 3a and Table S2). Furthermore, the TEM image clearly showed that gold nanoparticle-labeled NCa[10a,12] (Au-NCa) (Table S2) was well-decorated onto the NCl surface (Figure 3a).

The release profiles of DOX from DOX/NCl/NCa at different pH values were determined[8a] (Figure 3b), and pH reduction resulted in promoted release of DOX. At pH 5.4, the cumulative release of DOX within 260 min was 3.7-fold that at pH 7.4. In contrast, there was no apparent difference in the release of DOX from DOX/NCl/cNCa at pH 5.4 and 7.4. Similarly, The NCl/NCa complexes remained stable at pH 7.4 for 2 h, while a high degradation efficiency of NCl/NCa complexes was observed at pH 5.4 (Figure 3c).

To enhance the tumor-targeting efficacy of DOX/NCl/NCa, a ligand containing FA (cDNA-PEG-FA) was hybridized into the NCl, and the hybridization of cDNA-PEG-FA to the NCl resulted in no significant change in the NCl particle size and ζ potential (Table S2). The endocytosis pathway of DOX/FA-NCl/NCa was determined by incubating human breast cancer (MCF-7) cells overexpressing FR[13] with different inhibitors for specific pathways (Figure 4a). Compared with other inhibitors, both chlorpromazine (CPZ) and amiloride (AMI) displayed pronounced effects in inhibiting the internalization of DOX/FA-NCl/NCa, suggesting that DOX/FA-NCl/NCa was internalized by the cells and localized in the acidic endosomes.

dx.doi.org/10.1021/ja5088024 | J. Am. Chem. Soc. 2014, 136, 14722−14725

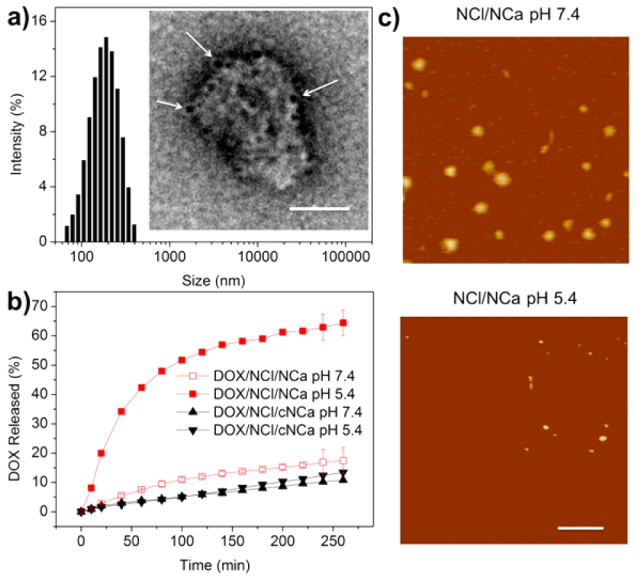

Figure 3. (a) Hydrodynamic size of NCl/NCa complexes. Inset: TEM image of an NCl/Au-NCa complex. The scale bar is 100 nm. The arrows indicate Au-NCa adsorbed on the NCl surface. (b) DOX release from DOX/NCl/NCa and DOX/NCl/cNCa at pH 7.4 and 5.4. Bars represent mean ± SD (n = 3). (c) AFM images of NCl/NCa complexes after incubation at pH 7.4 and 5.4 for 2 h. The scale bar is 500 nm.

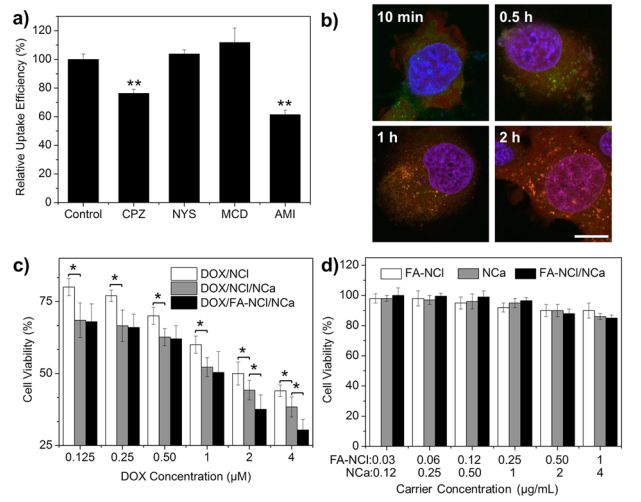

Figure 4. (a) Relative uptake efficiency of DOX/FA-NCl/NCa by MCF-7 cells. **, P < 0.01 compared with the control. Bars represent mean ± SD (n = 3). (b) Confocal laser scanning microscopy images of MCF-7 cells after incubation with DOX/FA-NCl/NCa for different times. Late endosome and lysosomes were stained with LysoTracker green. Red, DOX; green, endolysosome; blue, Hoechst 33342; yellow, colocalization of red and green pixels; magenta, colocalization of red and blue pixels. The scale bar is 10 μm. (c) In vitro cytotoxicities of DOX/NCl, DOX/NCl/NCa, and DOX/FA-NCl/NCa against MCF-7 cells for 24 h. *, P < 0.05. Bars represent mean ± SD (n = 6). (d) In vitro cytotoxicities of the blank FA-NCl, NCa, and FA-NCl/NCa against MCF-7 cells for 24 h. Bars represent mean ± SD (n = 6).

The intracellular distribution of DOX/FA-NCl/NCa was then detected (Figures 4b and S6). The internalization and nucleus targeting of DOX/FA-NCl/NCa in MCF-7 cells was extremely fast even within the first 10−30 min, during which period obvious endolysosomal entrapment and nucleus targeting of DOX could be observed. Colocalization of DOX/FA-NCl with NCa in MCF-7 cells was also observed (Figure S7). In the first 10 min, DOX/FA-NCl/AF488-NCa was internalized together. The fluorescence signals of DOX and AF488 showed a high colocalization. After 0.5 h, a large amount of DOX was released from the DOX/FA-NCl/AF488-NCa into the cytosol and specifically accumulated in the nucleus. Such rapid cytosolic distribution and nucleus-targeting effects of DOX delivered by DOX/FA-NCl/NCa were attributed to the efficient degradation of DOX/FA-NCl by NCa to promote the release of DOX.

The in vitro cytotoxicities of DOX/NCl, DOX/NCl/NCa, and DOX/FA-NCl/NCa against MCF-7 cells were estimated (Figure 4c). DOX/NCl/NCa showed a remarkably higher cytotoxicity toward MCF-7 cells than DOX/NCl. The half-maximal inhibitory concentration (IC_{50}) of DOX/NCl/NCa was calculated to be 1.2 μM, which is noticeably lower than the value of 2.3 μM for DOX/NCl. This verified that the NCa-mediated DOX release increased the toxicity of DOX delivered by NCl. This was further validated by the significantly higher cytotoxicity of MCF-7 treated with DOX/NCl/NCa than that associated with DOX/NCl/cNCa (Figure S8). Additionally, the conjugation of FA onto the NCl surface enhanced the therapeutic efficacy of DOX (Figure 4c). DOX/FA-NCl/NCa had the lowest IC_{50} (0.9 μM) compared with both DOX/NCl/NCa and DOX/NCl. The blank FA-NCl without DOX showed negligible toxicity at all tested concentrations (Figure 4d). It is noteworthy that although DNase I, the component of the carrier in this research, has been used as an anticancer agent in some other studies,[14] the cytotoxicity of NCa toward MCF-7 at the selected concentration in this study was compromised compared with that of released DOX (Figure 4d).

In summary, we have developed a bioinspired self-degradable drug delivery system consisting of a woven DNA "nanoclew" as a "cocoon matrix" and a "caged" DNase I nanogel as "hibernating worms". The "worms" can be readily activated to degrade their cocoon to release encapsulated drugs in the endolysosomal compartments. We will further the evaluate in vivo anticancer efficacy and biocompatibility of this delivery system. Our unique strategy provides insights for the design of new prodrugs and can be further extended to engineer other programmed drug delivery systems.

■ ASSOCIATED CONTENT

Supporting Information

Experimental procedures and characterization of the nanoparticles. This material is available free of charge via the Internet at http://pubs.acs.org.

■ AUTHOR INFORMATION

Corresponding Authors

zgu@email.unc.edu or zgu3@ncsu.edu
rmo@cpu.edu.cn

Notes

The authors declare no competing financial interest.

■ ACKNOWLEDGMENTS

This work was supported by the grant from NC TraCS, NIH's Clinical and Translational Science Awards (CTSA, 1UL1TR001111) at UNC-CH, the NC State Faculty Research and Professional Development Award, and the start-up package

from the Joint BME Department of UNC-CH and NCSU to Z.G.

REFERENCES

(1) (a) Lee, H.; Lytton-Jean, A. K. R.; Chen, Y.; Love, K. T.; Park, A. I.; Karagiannis, E. D.; Sehgal, A.; Querbes, W.; Zurenko, C. S.; Jayaraman, M.; Peng, C. G.; Charisse, K.; Borodovsky, A.; Manoharan, M.; Donahoe, J. S.; Truelove, J.; Nahrendorf, M.; Langer, R.; Anderson, D. G. *Nat. Nanotechnol.* **2012**, *7*, 389−393. (b) Douglas, S. M.; Bachelet, I.; Church, G. M. *Science* **2012**, *335*, 831−834. (c) Andersen, E. S.; Dong, M.; Nielsen, M. M.; Jahn, K.; Subramani, R.; Mamdouh, W.; Golas, M. M.; Sander, B.; Stark, H.; Oliveira, C. L. P.; Pedersen, J. S.; Birkedal, V.; Besenbacher, F.; Gothelf, K. V.; Kjems, J. *Nature* **2009**, *459*, 73−76. (d) Zhang, Z.; Eckert, M. A.; Ali, M. M.; Liu, L.; Kang, D.-K.; Chang, E.; Pone, E. J.; Sender, L. S.; Fruman, D. A.; Zhao, W. *ChemBioChem* **2014**, *15*, 1268−1273. (e) Lo, P. K.; Karam, P.; Aldaye, F. A.; McLaughlin, C. K.; Hamblin, G. D.; Cosa, G.; Sleiman, H. F. *Nat. Chem.* **2010**, *2*, 319−328. (f) Zhang, Z.; Ali, M. M.; Eckert, M. A.; Kang, D.-K.; Chen, Y. Y.; Sender, L. S.; Fruman, D. A.; Zhao, W. *Biomaterials* **2013**, *34*, 9728−9735. (g) Zhu, G.; Hu, R.; Zhao, Z.; Chen, Z.; Zhang, X.; Tan, W. *J. Am. Chem. Soc.* **2013**, *135*, 16438−16445. (h) Hu, R.; Zhang, X.; Zhao, Z.; Zhu, G.; Chen, T.; Fu, T.; Tan, W. *Angew. Chem., Int. Ed.* **2014**, *53*, 5821−5826.

(2) (a) Kim, K.-R.; Kim, D.-R.; Lee, T.; Yhee, J. Y.; Kim, B.-S.; Kwon, I. C.; Ahn, D.-R. *Chem. Commun.* **2013**, *49*, 2010−2012. (b) Zhao, Y.-X.; Shaw, A.; Zeng, X.; Benson, E.; Nyström, A. M.; Högberg, B. *ACS Nano* **2012**, *6*, 8684−8691.

(3) Lee, J. B.; Hong, J.; Bonner, D. K.; Poon, Z.; Hammond, P. T. *Nat. Mater.* **2012**, *11*, 316−322.

(4) (a) Schüller, V. J.; Heidegger, S.; Sandholzer, N.; Nickels, P. C.; Suhartha, N. A.; Endres, S.; Bourquin, C.; Liedl, T. *ACS Nano* **2011**, *5*, 9696−9702. (b) Li, J.; Pei, H.; Zhu, B.; Liang, L.; Wei, M.; He, Y.; Chen, N.; Li, D.; Huang, Q.; Fan, C. *ACS Nano* **2011**, *5*, 8783−8789.

(5) Wang, K.; You, M.; Chen, Y.; Han, D.; Zhu, Z.; Huang, J.; Williams, K.; Yang, C. J.; Tan, W. *Angew. Chem., Int. Ed.* **2011**, *50*, 6098−6101.

(6) (a) Xiao, Z.; Ji, C.; Shi, J.; Pridgen, E. M.; Frieder, J.; Wu, J.; Farokhzad, O. C. *Angew. Chem., Int. Ed.* **2012**, *51*, 11853−11857. (b) Zhang, Z.; Che, Y.; Smaldone, R. A.; Xu, M.; Bunes, B. R.; Moore, J. S.; Zang, L. *J. Am. Chem. Soc.* **2010**, *132*, 14113−14117.

(7) (a) Peer, D.; Karp, J. M.; Hong, S.; Farokhzad, O. C.; Margalit, R.; Langer, R. *Nat. Nanotechnol.* **2007**, *2*, 751−760. (b) Shi, J.; Votruba, A. R.; Farokhzad, O. C.; Langer, R. *Nano Lett.* **2010**, *10*, 3223−3230. (c) Chow, E. K.-H.; Ho, D. *Sci. Transl. Med.* **2013**, *5*, No. 216rv214.

(8) (a) Mo, R.; Jiang, T.; DiSanto, R.; Tai, W.; Gu, Z. *Nat. Commun.* **2014**, *5*, 3364. (b) Mo, R.; Jiang, T.; Gu, Z. *Angew. Chem., Int. Ed.* **2014**, *53*, 5925−5930.

(9) Ali, M. M.; Li, F.; Zhang, Z.; Zhang, K.; Kang, D.-K.; Ankrum, J. A.; Le, X. C.; Zhao, W. *Chem. Soc. Rev.* **2014**, *43*, 3324−3341.

(10) (a) Yan, M.; Du, J.; Gu, Z.; Liang, M.; Hu, Y.; Zhang, W.; Priceman, S.; Wu, L.; Zhou, Z. H.; Liu, Z.; Segura, T.; Tang, Y.; Lu, Y. *Nat. Nanotechnol.* **2010**, *5*, 48−53. (b) Gu, Z.; Yan, M.; Hu, B.; Joo, K.-I.; Biswas, A.; Huang, Y.; Lu, Y.; Wang, P.; Tang, Y. *Nano Lett.* **2009**, *9*, 4533−4538.

(11) (a) Murthy, N.; Thng, Y. X.; Schuck, S.; Xu, M. C.; Fréchet, J. M. J. *J. Am. Chem. Soc.* **2002**, *124*, 12398−12399. (b) Murthy, N.; Xu, M.; Schuck, S.; Kunisawa, J.; Shastri, N.; Fréchet, J. M. J. *Proc. Natl. Acad. Sci. U.S.A.* **2003**, *100*, 4995−5000. (c) Bachelder, E. M.; Beaudette, T. T.; Broaders, K. E.; Dashe, J.; Fréchet, J. M. J. *J. Am. Chem. Soc.* **2008**, *130*, 10494−10495.

(12) Liu, Y.; Du, J.; Yan, M.; Lau, M. Y.; Hu, J.; Han, H.; Yang, O. O.; Liang, S.; Wei, W.; Wang, H.; Li, J.; Zhu, X.; Shi, L.; Chen, W.; Ji, C.; Lu, Y. *Nat. Nanotechnol.* **2013**, *8*, 187−192.

(13) Li, K.; Jiang, Y.; Ding, D.; Zhang, X.; Liu, Y.; Hua, J.; Feng, S.-S.; Liu, B. *Chem. Commun.* **2011**, *47*, 7323−7325.

(14) Alcazar-Leyva, S.; Ceron, E.; Masso, F.; Montano, L. F.; Gorocica, P.; Alvarado-Vasquez, N. *Med. Sci. Monit.* **2009**, *15*, CR51−CR55.